Phosphorescence Control Mediated by Molecular Rotation and Aurophilic Interactions in Amphidynamic Crystals of 1,4-bis[tri-(*p*-fluorophenyl)phosphane-gold(I)-ethynyl]benzene

Mingoo Jin,[‡] Tim S. Chung,[†] Tomohiro Seki,[‡] Hajime Ito,*[‡] and Miguel A. Garcia-Garibay*[†]

[‡]Division of Applied Chemistry and Frontier Chemistry Center (FCC), Faculty of Engineering, Hokkaido University, Sapporo, Hokkai-do 060-8628, Japan

[†]Department of Chemistry and Biochemistry, University of California Los Angeles, California 90095-1569, United States

Molecular rotor, Amphydynamic crystal, Luminescent gold(I) complex

ABSTRACT: Here we present a structural design aimed at the control of phosphorescence emission as the result of changes in molecular rotation in a crystalline material. The proposed strategy includes the use of aurophilic interactions, both as a crystal engineering tool and as sensitive emission probe, and the use of a dumbbell-shaped architecture intended to create a low packing density region that permits the rotation of a central phenylene. Molecular rotor **1** with of a central 1,4-diethynylphenylene rotator linked to two gold(I) triphenylphosphane complexes was prepared and its structure confirmed by single crystal X-ray diffraction (XRD), which revealed chains mediated by dimeric aurophilic interactions. We showed that green emitting crystals exhibit reversible luminescent color changes between 298 K to 193 K, which correlate with changes in rotational motion determined by variable temperature (VT) solid state (SS) ^{2}H NMR spin-echo experiments. Fast 2-fold rotation with a frequency of ca. 4.00 MHz (τ=0.25 μs) at 298 K becomes essentially static below 193 K as emission steadily changes from green to yellow in this temperature interval. A correlation between phosphorescence lifetimes and rotational frequencies is interpreted in terms of conformational changes arising from rotation of the central phenylene, which causes a change in electronic communication between the gold-linked rotors, as suggested by DFT studies. These results and control experiments with analog **2** possessing a hindered tetra-methylphenylene that is unable to rotate in the crystal suggest that the molecular rotation can be a useful tool for controlling luminescence in the crystalline state.

Introduction

The precise control of luminescent properties in solid-state materials has attracted much attention because of their potential for the development of sophisticated functional materials such as sensors, transducers and external field-sensitive devices.[1] A concept that has attracted a great deal of attention in this context is the development of aggregation induced emission (AIE), pioneered by Tang and co-workers. In this case, it has been shown that the rotation of conjugated groups within certain chromophores result in emission quenching as the excited state is able to decay through a conical intersection (CI).[2] Therefore, while the AIE chromophores are non-emissive and are free to explore their torsional space in solution, aggregation and crystallization suppress their rotational freedom and prevents access to the CI, such that emission can be turned on in the solid state.

In order to further develop the field of functional luminescent materials, in addition to having binary systems with one state described by molecules that are free to rotate in solution and another one where molecules are aggregated in the solid state, it would be advantageous to control luminescence efficiency by affecting the rate of rotation in the solid state.[3] To accomplish that, we propose the use of amphidynamic crystals based on elements of molecular and crystal engineering to produce materials that combine luminescence and rotational motion.[4] In fact, several previous reports have described amphidynamic crystals[4] with a *p*-phenylene moiety linked by two triple bonds exhibiting rotational motion in the solid state.[4a c,j,k] One of the most robust and general architectures for the formation amphidynamic molecular crystals is based on the use of dumbbell shaped molecular rotors, as illustrated in Figure 1a and 1b.[5] These molecular *rotors* consist of a central phenylene *rotator* (shown in red) that is axially linked by triple bonds, or *axle*, to two bulky groups that play the role of a *stator* (shown blue in Figure 1b). These structures are able to generate crystals with a relatively low packing density near the zone of the rotator in an otherwise densely-packed environment. For the objectives of this work, we recognized that the luminescence of crystalline gold(I) complexes can be highly sensitive to external stimuli, such as exposure to solvent vapor, changes in temperature, and mechanical stress, which often result in large changes in emission properties.[6] It is well known that these changes are the result of subtle structural changes around the gold complexes, which are highly sensitive to their environment, primarily as a result of their large and highly polarizable *d*-orbitals. Thus, their electronic environment can easily be influenced by internal or external changes, molecular conformations, the dipole moment of

neighboring systems, and alternative molecular arrangements.[6] Furthermore, a tendency to form aurophilic interactions (Au–Au < 3.5 Å) can be used both as a crystal engineering synthon and as an emission tool with higher emission intensities and lower HOMO-LUMO energy gap.[7]

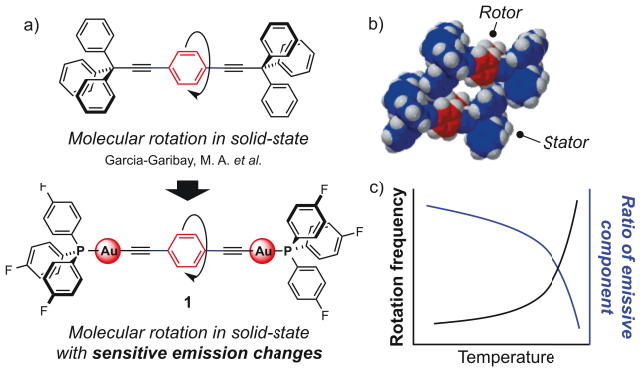

Figure 1. a) Molecular design based on the substitution of the triphenylmethane by a triarylphosphane gold(I) complex in a 1,4-bis(triphenylpropynyl)benzene. b) The dumbbell shaped molecular rotors with *rotor* and *stator* indicates in the crystal. c) Expected relation between rotation frequency and emission properties.

Taking dumbbell shaped molecular rotors as a model structure, we decided to incorporate the desired gold(I) atoms by taking advantage of complexation with the *p*-dialkynylphenylene rotator and a tri-(*p*-fluorophenyl)phosphane stator to form gold complex **1** in Figure 1 and Scheme 1 (R=H). Analog **2** (Scheme 1, R=Me), with a hindered *p*-dialkynyl-tetramethylphenylene that is unable to rotate in the crystal was also prepared to conduct control experiments. With these structures, we set out to (1) expand the scope of amphidynamic materials using gold(I) complexes, (2) determine changes in emission properties in terms of rotational frequencies as a function of temperature, and (3) look for a possible correlation between emission and rotational frequency. We hypothesized that rotational motion in crystals of **1** would be relatively fast at high temperatures, which would lead to emission quenching while low temperatures should slow down the molecular rotor allowing for higher emission (Figure 1c). By contrast, we expected crystals of **2** with a static tetra-methylphenylene to show no changes in emission as a function of temperature. As described below, the general concepts formulated for this work were realized. The desired structures were obtained, changes in emission and rotational motion in the case of **1** were observed as a function of temperature, and a general correlation such as that predicted in Figure 1c was observed.

RESULTS AND DISCUSSION

Synthesis and Characterization. Dumbbell-shaped gold complexes **1**, **1-*d*$_4$ and 2** were synthesized from derivatives of 1,4-diethynylbenzene and tris(4-fluorophenyl)phosphane gold(I) chloride using standard alkynylation conditions, as illustrated in Scheme 1.[8] Crystallization was accomplished by layering hexane as a poor solvent on top of a solution of the rotor complex in chloroform (typically, 10 mg of the complex in 2 ml of chloroform), which afforded green yellowish crystals (below 0.3 mm in size) subsequently shown to emit green light. No solvent inclusion was observed by either X-Ray diffraction or thermogravimetric analysis (TGA) (Figure S1). The samples were characterized by ^{1}H and ^{13}C nuclear magnetic resonance (NMR) spectroscopy, high-resolution mass spectrometry, elemental analysis, TGA, and single crystal X-ray diffraction (XRD) analyses (see the Supporting Information).

Scheme 1.

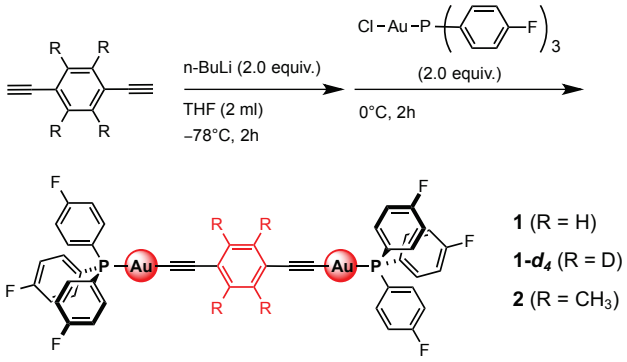

Single Crystal X-Ray Diffraction and Thermal Analyses of 1 and 2. To obtain precise structural information, we performed single crystal XRD analysis of complexes **1** and **2**. Gold(I) complex **1** crystallized in the triclinic space group *P*-1 with two distinct half molecules per asymmetric unit, each occupying a crystallographic inversion center, so that two full molecules are generated per unit cell (Z=2) (Table S1). The desired structure was confirmed, as illustrated in Figure 2a, and the expected inter-molecular aurophilic interactions between neighboring molecules (Au–Au distance: 3.05 Å) were shown to occur as dimers (Figure 2b). Phenylene rotators are surrounded by fluorophenyl groups from the phosphane stators of neighboring molecular rotors displaying T-shaped CH-π interaction (Figure 2b). Interestingly, two dimeric aurophilic interactions at the ends of the central diethynyl benzene lead to the formation of infinite zigzag chains, as shown in Figure 2c and S2.

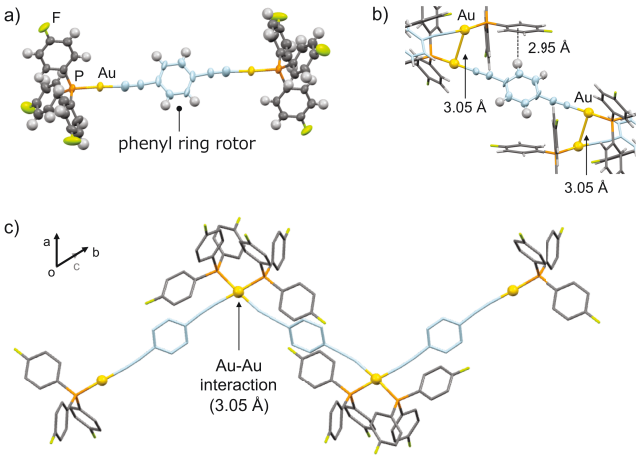

Figure 2. a) Structure of dinuclear gold(I) complex **1** at 123 K. b) Dimeric aurophilic interactions between neighboring molecular rotors. c) Zig-zag chains of molecular rotors formed by dimeric aurophilic interactions.

Gold(I) complex **2** with a bulky tetramethyl benzene group was prepared to investigate the emission properties of an

isostructural non-rotating structure (Figure 3a). Crystals of **2** were obtained in the monoclinic space group *C*2/*c* with several characteristics that are common to those found in crystals of **1** (Table S1). There are two distinct half molecules per asymmetric unit with coinciding molecular and crystallographic inversion centers, such that there are two sets of four crystallographically distinct molecules per unit cell (*Z*=8) (Table S1). While the crystal system and packing structure of **2** are different from those of **1**, they have similar intermolecular aurophilic interactions with neighboring molecules experiencing Au–Au distances of 3.36 Å, as shown in Figure 3b. The tetramethyl phenylene rotator of **2** is surrounded by the fluorophenyl groups of neighboring stators, but in this case presenting nearly parallel π–π interactions (Figure 3b), instead of the CH-π interactions observed in the case of **1** (Figure 2b). The robust nature of these supramolecular crystal-guiding interactions was also shown by the formation of intermolecular zig-zag chains that are very similar to those in crystal **1** (Figure 3c and S3–4), except that tetramethyl phenyl rotator **2** is more densely packed and less likely to display fast molecular rotation (Figure 3c and S3).

Single crystal XRD data were collected for both crystals in the range 123–298 K with five intermediate steps (193, 213, 233, 253, and 273 K). No phase transitions and no collapse of the intermolecular networks were observed, with only small changes in crystal dimensions and volume noted (Figure S5–S9 and Table S1). Differential scanning calorimetry (DSC) profiles of the crystal **1** and **2** showed no peaks in the range 193–298 K, indicating that there are no phase transitions in this temperature range (Figure S10). The experimental powder XRD of samples of **1** and **2** exhibited the same patterns as compared to those obtained by simulationd from the single crystal diffraction data (Figure S11). This indicates that the powder samples are in fact crystalline and form the same polymorph as single crystal specimens.

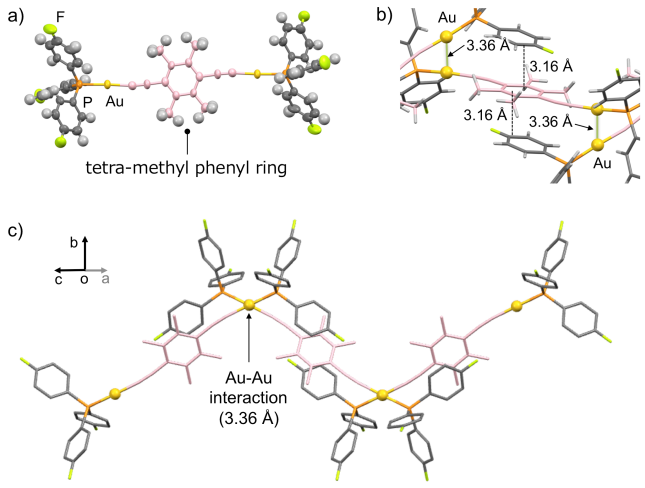

Figure 3. a) Structure of dinuclear gold(I) complex **2** at 123 K. b) Dimeric aurophilic interactions between neighboring molecules. c) Zig-zag chains of molecular rotors formed by dimeric aurophilic interactions.

Variable Temperature Solid State NMR Experiments of 1-*d*$_4$ and 2. In order to investigate the rotational dynamics of gold(I) rotor **1**, we performed solid state (SS) ^{2}H NMR spin-echo measurements and line shape simulations. This is a relatively simple and widely used technique to analyze internal dynamics of deuterium-enriched groups in the dynamic window of 10^3–10^8 Hz.[9] The variable temperature (VT) SS ^{2}H NMR spin-echo measurements were performed on polycrystalline powders of **1-*d*$_4$** to determine the rotational frequency of the central phenylene rotator as a function of temperature.

Figure 4a and S12 shows the experimental line shapes observed in the temperature range between 318 and 193 K in solid black lines. The line shapes obtained by simulation provided a reasonably good match with those obtained in the experiment (red dotted lines) using a quadrupolar coupling constant (QCC) of 180 kHz,[9] characteristic of aromatic deuterons, a cone angle of 60° formed between the rotational axis and C-D bond vector, and Brownian jumps of 180° about a two-fold potential energy profile, in agreement with the crystal structure where two degenerate minima can be expected. Line shape simulations required site exchange frequencies that expand the entire dynamic range of the method.[5a] The line shape at 318 K is close to the fast exchange regime and a good match was obtained with a 12.5 MHz rotational frequency. At ambient temperature (298 K), the line shape suggests rotational motion in the intermediate exchange regime with a frequency of ca. 4.0 MHz. The experimental spectra measured at temperatures of 273, 253, 233, 213, and 193 K, were simulated with rotational exchange frequencies of ca. 2.50, 1.41, 0.35, 0.15, and below 0.01 MHz, respectively. An Arrhenius plot constructed from the rotational exchange frequencies for **1-*d*$_4$** (Figure 4b) indicates a relatively low activation energy of E_a = 5.21 kcal/mol and a pre-exponential factor of $A = 5.8 \times 10^{10}$ s^{-1}, which is somewhat smaller that the value expected for an elementary torsional mode of ca. 10^{12} s^{-1}.

Expecting a much slower rotational motion for the tetramethyl phenylene rotator of **2** we decided to explore its motion using VT ^{13}C CPMAS (Figure 4c and S13). This experiment is analogous to VT measurements carried out in solution where signals broaden, coalesce, collapse, and sharpen as the rate of site exchange changes from much slower to much faster than the value corresponding to the chemical shift difference between the exchanging groups. For that reason, the dynamic range of the method is relatively slow and generally limited to site exchange in the ca. 10–10^4 Hz. The temperature range explored for the VT CPMAS ^{13}C NMR experiment was the same as that analyzed in the VT SS ^{2}H NMR spin-echo experiment for **1-*d*$_4$**, between 318 K and 193 K. We assigned the resonance signals of methyl groups in the hindered rotator moiety to peaks observed at ca. 16–18 ppm, which are marked with an asterisk in Figure 4c. It should be noted that methyl groups related by 180° rotation in **2** are expected to have different chemical shifts as a result of their crystallographically and magnetically different environments. Notably, there was no change in the width or position of the methyl group signals at 16 and 18 ppm as a function of temperature, indicating that there is no rotational site exchange in the dynamic range given by their frequency difference of Δν = 300 Hz (coalescence would occur at a rate of ca. k = 2.22 x 300 Hz = 666 Hz). As illustrated in Figure 4d, we conclude that the time constant for rotational motion of the phenylene rotator in crystals of **1** at ambient temperature (ca. 0.25 μs) should be in reasonable proximity to the time constants which are typical in the phosphorescence time window (see below). By contrast, the tetramethyl phenylene rotator of **2** is essentially static, even at the highest temperatures analyzed.

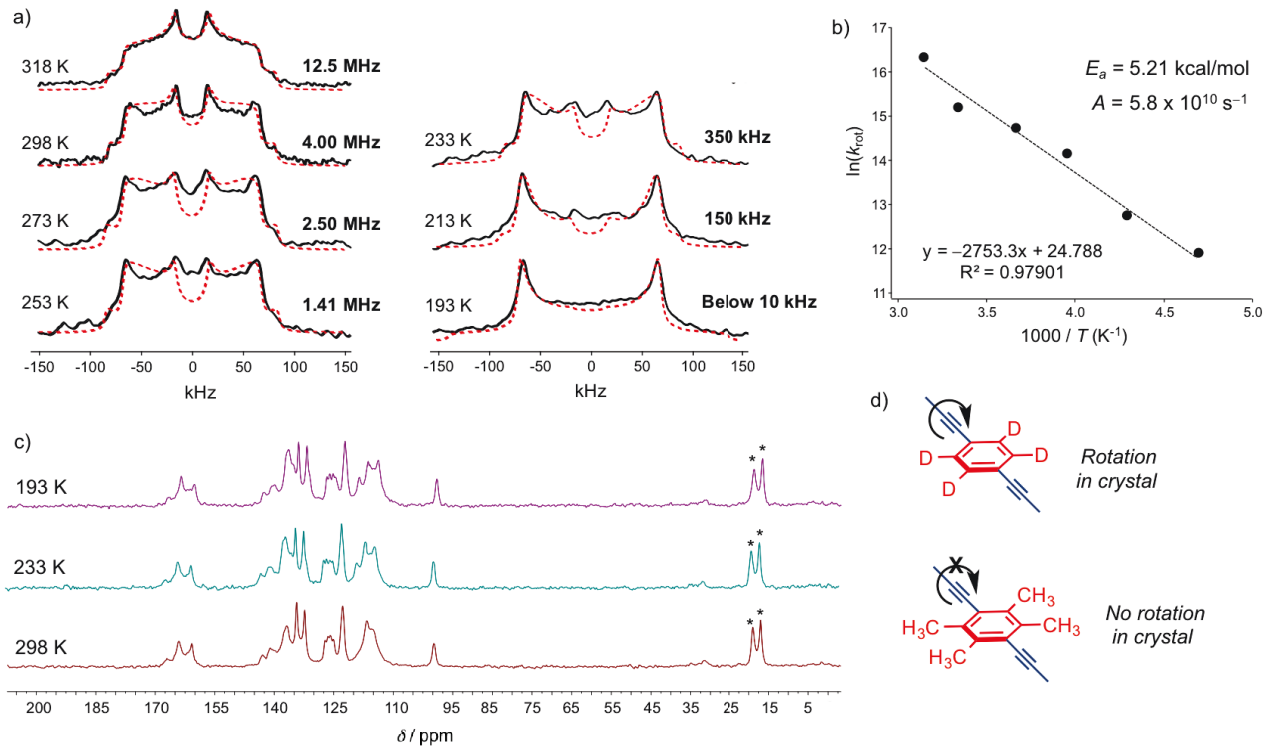

Figure 4. Variable temperature (VT) solid-state (SS) NMR studies of **1** and **2**. a) Experimental (black solid line) and simulated (red dashed line) SS ^{2}H NMR spectra of crystal **1**. b) Arrhenius plot of phenyl ring rotor dynamics in crystal **1**. c) SS ^{13}C CPMAS spectra of crystal **2** acquired at 150 MHz. * indicates peaks from the methyl group of tetra-methyl phenyl moiety. d) Schematic representation of the results of VT SS NMR studies of **1** and **2**.

Emission properties of 1 and 2. Crystalline samples of complexes **1** and **2** were found to exhibit green and yellow emission, respectively, under UV light excitation (λ_{ex} = 370 nm) at 298 K (Figures 5a and 6a). The emission intensities of **1** and **2** in dilute $CHCl_3$ solution were very weak as compared to those in the solid state (Figure S14-15), as expected for a long-lived triplet emission that is highly susceptible to quenching.[10] Complex emission lifetimes in the microsecond regime described below confirmed that the crystalline state emission can be assigned as phosphorescence. Crystal **1** showed reversible visual changes in emission from green to yellow as the temperature changes from 298 to 193 K (Figure 5a). The temperature range of these changes matches well the temperature range where the thermally activated molecular rotator varies from highly dynamic to nearly static. The emission spectrum of **1** consists of a sharp, well resolved peak at 498 nm, followed by a several less resolved peaks and shoulders with a λ_{max} = 543 nm, suggesting a relatively rich vibronic structure. Lowering the temperature from 298 to 193 K resulted in the relative increase in intensity of the lower energy bands, which is responsible for the visual changes in emission going from green to yellow (Figure 5b).

The solid state emission of the static molecular rotor **2** shown in Figure 6 does not have the vibrational resolution of the unsubstituted compound, and there are no visual or spectral changes as a function of temperature from 298 K to 193K. The spectrum has a λ_{max} = 545 nm with an envelop that spans from ca. 490 nm to 700 nm, covering the same energy range as **1**, but lacking a strong 0-0 transition and displaying significant broadening of the lower energy bands. To suggest an explanation for the observations shown in Figure 5 and 6, we propose assignments for the emissions of **1** and **2**, consider the photophysical properties of conjugated arylene-ethynylenes as a function of rotation, and explore the role of the gold(I) centers in the electronic communication among the diethynylphenylene rotors in the crystal.

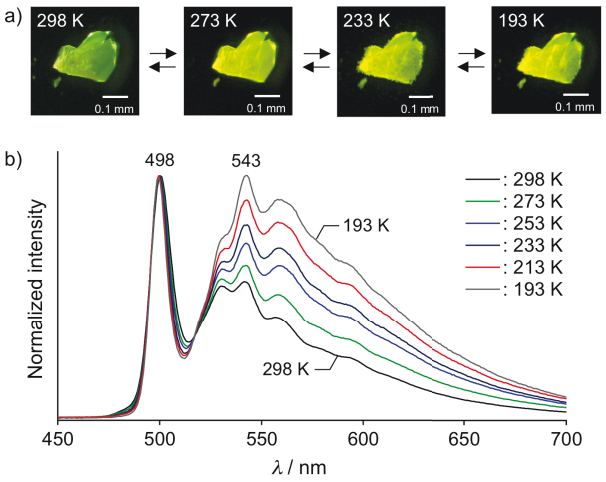

Figure 5. a) Photographs of emission color changes of **1** under UV irradiation by cooling or heating. b) Emission spectra of **1** in various temperatures.

We first note that the emission spectrum of **1** is consistent with the phosphorescence of an isolated π-conjugated di-

ethynyl arene chromophore.[10,11] This includes a vibronic structure that includes a strong 0-0 transition and a rich vibrational progression that arises from several C-H stretching and bending modes.[10,12] The spectrum of **2**, by contrast, is consistent with a similar diethynyl arene chromophore under conditions of co-facial aggregation,[12,14] which tends decrease the intensity of the 0-0 band while broadening the rest of the spectrum.[12,14] These assignments are also consistent with structural parameters available from the corresponding crystal structures, which show the central aromatic ring to have a T-shaped C-H-π interaction with neighboring molecules in the case of **1** and co-facial π–π interactions in the case of **2**.

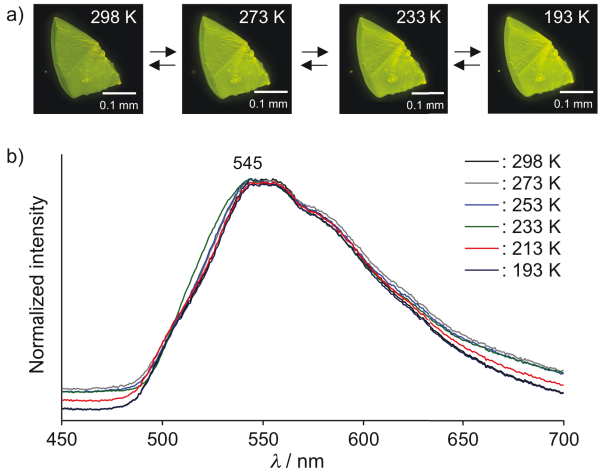

Figure 6. a) Photographs of no emission color changes of **2** under UV irradiation. b) Emission spectra of **2** in various temperatures.

Spectral changes as a function of rotational angle have been well documented for π-conjugated chromophores that are linked by triple bonds, such as tolane,[13] bis(phenylethynyl)benzene (Scheme 2a),[12,14] and numerous structures where electronic interactions are determined by metal centers.[10b-c,15] While rotation of aromatic groups relative to each other does not affect the ground state potential energy profile, electronic excitation causes changes in bond order with single and triple bonds acquiring cumulene character, which makes the excited state energies sensitive to twist angles of arene groups.[12,14] Thus, coplanar structures are fully delocalized in the ground and excited states (shown in red in the top frame of Scheme 2a), such that they tend to absorb and emit at lower energies as compared to the analogous twisted structures. In fact, twisting restricts conjugation in the excited state (Scheme 2a, bottom frame) so that those structures have greater excitation energies. Differences in the twist angle result in differences in the position of the spectrum, and in the relative intensity of the vibronic components, as shown with several linearly conjugated chromophores,[10,12] including a series of pentiptycenes that illustrate this effect remarkably well.[16] Another key feature of the π-conjugated chromophores is that phosphorescence tends to be more efficient from the twisted structures, which tend have an efficient intersystem crossing mechanism that leads to the population of the phosphorescent state.[13,16]

In order to extend the model shown in Scheme 2a to a chromophores such as the diethynylbenzene of **1** with a single aromatic group flanked by triple bonds that are coordinated to metal centers, we propose to take advantage of electronic interactions between neighboring molecular rotors that are made possible by Au–Au contacts. As shown in the top frame of Scheme 2b, we propose that parallel orbital alignment between the Au–Au bond and the π-system of the central aromatic phenylene can delocalize the wave function beyond a single chromophore, such that excitation in conformers with parallel aromatic rings can be shared between adjacent rotors, as illustrated by red color in the top structure in Scheme 2b.

Scheme 2

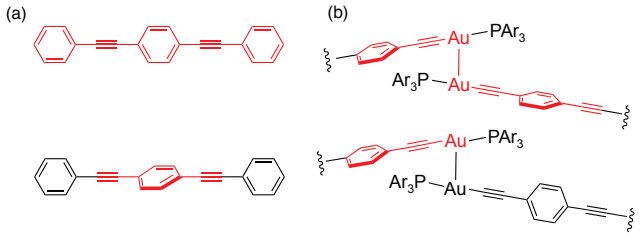

In order to test this hypothesis, we carried out time-dependent (TD) DFT calculations using a dimer with coordinates taken from single-crystal structure of **1** at 193 K (Figure 7, S16–17, and Table S2–5). The results of these calculations confirm that rotation of the phenyl ring within the reference frame given by the direction of the Au–Au bond of adjacent complexes can affect their electronic communication (Figure 7 and S17). In addition to the equilibrium geometry of the test Au–Au dimer present in the crystal, we carried out B3LYP/SDD calculations with a model where the central phenylenes were rotated by 90° (Table S3–4). The excitation energy calculated for the crystal structure had a relatively good agreement with the value obtained from the experimental phosphorescence excitation spectrum (Figure S16). Furthermore, the frontier molecular orbitals for the dimer with the crystal conformation indicated that the HOMO was distributed over the two diethynylbenzenes with a small density localized in the gold atoms of the dimer (Figure 7 and S17).[17] On the other hand, the HOMO of the dimer with the phenyl rings rotated by 90° was localized on a diethynylbenzene monomer, which is very similar to the bottom structure in Scheme 2b.

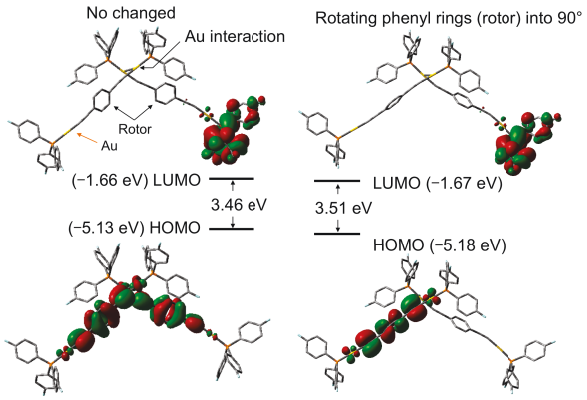

Figure 7. Frontier molecular orbitals and the corresponding energy levels obtained by TD-DFT calculations (B3LYP/SDD, singlet) of dimer in the crystal structures of **1** (left) and 90° rotated phenyl ring geometry (right).

The LUMOs of the two structures were mainly located on the tris(4-fluorophenyl)phosphane moiety in the complex (Figure 7 and S17). Furthermore, the HOMO-LUMO gaps were significantly different, suggesting that the two extreme structures should have distinct absorption and emission spectra. Results from calculations performed using a dimer of hindered rotor **2** were analogous to those from **1** (Figure S17 and Table S5), suggesting that changes in emission would also take place in **2** if rotation of the central tetra-methylphenylenes were possible in the corresponding crystals.

Potential correlation between triplet decay and rotational dynamics. In search of a qualitative correlation between the emission changes of **1** and the rotational frequency determined by solid-state NMR, we measured the phosphorescence decays of crystalline **1** and **2** at 498 and 543 nm at temperatures ranging from 195 to 298 K (Figure 8 and S18–19). The two data sets revealed high heterogeneities that depart significantly from single exponential functions with decays that span a time window from ca. 100-200 μs in the case of **1**, and ca. 2 ms in the case of **2**. Significantly, only the decay kinetics of dynamic rotors **1** displayed high temperature dependence and measurements carried out by detection at 498 and 543 nm resulted in different decays, highlighting the spectral heterogeneity and complexity of the solid state emission (Figure S18). Considering that reasonable decay models required multiple exponential functions with varying lifetimes (τ_n) and pre-exponentials (A_n), we calculated the weighted average from all the components for each sample ($\tau_{av} = \Sigma A_n \tau_n$) at every temperature, as shown for **1** in Table 1 and S6–7. Decay fits in the case of **2** (Table S8) require as many as four exponential functions leading to an average temperature-independent time constant of 56.6±7.5 μs. In the case of **1** we were able to use double exponential functions with varying pre-exponentials of short- (ca. 10 μs) and long-lived components (ca. 38 μs) in the temperature interval of 213–298 K (Table 1 and S6). However, measurements at 195 K required a small amount (ca. 10%) of an additional much longer component (110 μs, Table 1 and S6), which led to average time constants between ca. 11 μs to 32 μs in the range of 298 and 193 K. We note that excited state decay occurs within the range of the time constants for rotation (0.25 μs to 100 μs), which may help explain the high kinetic heterogeneity of the observed emission. One may visualize spectral changes in Figure 5 as resulting from a superposition of a vibrationally resolved spectrum of **1**, from a rotational minimum, combined with increasing contributions from a broad spectrum that arises from components experiencing increasingly large vibrations and rotational motion as the temperature increases.

While the data shown in Figures 5–8 support the role of phenylene rotation as the cause for the observed changes in emission, one should consider the fact that aurophilic interactions defined by Au–Au distances < 3.5 Å may also affect luminescent properties.[7] For example, the deformation of aurophilic interactions, which include changes in the Au–Au distance, can affect the delocalization and energetics of molecular orbitals, which in turn may also alter excitation energies and emission properties.[7] We found upon inspection of the XRD structures that changes in the Au–Au distances in the range of 193–298 K for **1** and **2** are not sufficient to explain the different trends in their corresponding emission properties

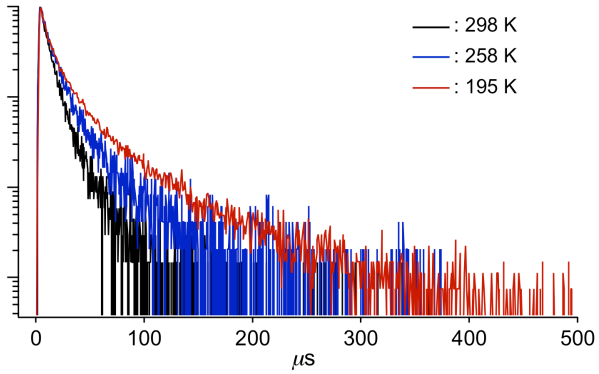

Figure 8. Emission decay of the crystalline **1** observed at 543 nm in various temperatures.

Table 1. Emission lifetimes of the crystalline 1 at 543 nm in various temperatures.[a]

Temp. / K	τ_1 (A_1) /μs (-)	τ_2 (A_2) /μs (-)	τ_3 (A_3) /μs (-)	τ_{av}[b] /μs
298	10.0 (0.95)	38.3 (0.05)	-	11.4
273	10.2 (0.91)	38.2 (0.09)	-	12.6
253	10.1 (0.73)	38.4 (0.27)	-	17.7
233	10.1 (0.67)	38.9 (0.33)	-	19.7
213	10.0 (0.61)	38.8 (0.39)	-	21.1
195	10.1 (0.49)	38.8 (0.41)	111.0 (0.10)	32.0

[a]Results from measurements obtained with crystals of **2** are included in table S8. [b] $\tau_{av} = \Sigma\, \tau_n\, A_n$, obtained by tail fitting (λ_{ex} = 370 nm).

(Figure S9). The Au–Au distances of **1** and **2** increased upon heating to 298 K, and their corresponding changes were 0.042 and 0.054 Å, respectively, with a greater change observed for the complex that presents no changes in emission. Based on these observations, we conclude that the phosphorescence changes upon cooling and heating are not correlated with aurophilic interactions but are more likely the result changes in electronic communication that occur when the central phenylene vibrates and rotates in the crystal.

Summary

In this work, we described the first example of a crystalline material where changes in phosphorescence appear to be the result of changes in the rotational motion of an aromatic chromophore that is part of dumbbell-shaped gold(I) complex **1.** Changes in emission properties and rotational frequency exhibited a reasonable correlation, and TD-DFT studies revealed that conformational changes of the phenylene rotator can cause changes in the electronic communication between adjacent chromophores. Furthermore, gold(I) complex **2** with a sterically hindered tetramethylphenylene rotator provided us with an excellent control sample where no changes in emission color and no rotational motion can be detected in its crystals. These results strongly indicate that the luminescence properties of bulk materials can be tuned by taking advantage of amphidynamic crystals that allow for structurally-controlled rotational motion.

ASSOCIATED CONTENT

Supporting Information. Spectroscopy, X-ray crystal graphic, thermal analysis, quantum chemical calculation data and other additional information. This material is available free of charge via the Internet at http://pubs.acs.org.

AUTHOR INFORMATION

Corresponding Author

hajito@eng.hokudai.ac.jp; mgg@chem.ucla.edu

Present Addresses

‡Kita 13 Nishi 8 Kita-ku, Sapporo, Hokkaido, 060-8628, Japan
†607 Charles E. Young Drive East, Los Angeles CA 90095-1569, USA

Author Contributions

All of the authors have given their approval to the final version of the manuscript.

ACKNOWLEDGMENT

This work was financially supported by the MEXT (Japan) program "Strategic Molecular and Materials Chemistry through Innovative Coupling Reactions" of Hokkaido University; Building of Consortia for the Development of Human Resources in Science and Technology, "Program for Fostering Researchers for the Next Generation"; the Ministry of Education, Culture, Sports, Science and Technology through a Program for Leading Graduate Schools (Hokkaido University "Ambitious Leader's Program"); and by JSPS KAKENHI grants JP15H03804, JP16H06034, JP17H05134, JP17H05344, and JP17H06370. Jin, M. was supported by the grant-in-aid for JSPS Fellows JP17J01104. We also thank the Frontier Chemistry Center Akira Suzuki "Laboratories for Future Creation" Project, Hokkaido University. Work at UCLA was made possible by National Science Foundation grant DMR1700471. We thank Dr. Salvador Perez-Estrada (UCLA) for valuable discussions.

REFERENCES

(1) (a) Yan, D.; Evans, D. G. *Mater. Horiz.* **2014**, *1*, 46. (b) Friend, R. H.; Gymer, R. W.; Holmes, A. B.; Burroughes J. H.; Marks, R. N. *Nature*, **1999**, *397*, 121. (c) Mutai, T.; Satou, H.; Araki, K. *Nat. Mater.* **2005**, *4*, 685. (d) Sagara, Y.; Yamane, S.; Mitani, M.; Weder, C.; Kato, T. *Adv. Mater.* **2016**, *28*, 977.
(2) Hong, Y.; Lam, J. W. Y.; Tang, B. Z. *Chem. Soc. Rev.* **2011**, *40*, 5361.
(3) (a) Shustova, N. B.; McCarthy, B. D.; Dincă, M. *J. Am. Chem. Soc.* **2011**, *133*, 20126. (b) Shustova, N. B.; Ong, T.-C.; Cozzolino, A. F.; Michalis, V. K.; Griffin, R. G.; Dincă, M. *J. Am. Chem. Soc.* **2012**, *134*, 15061. (c) Hughs, M.; Jimenez, M.; Khan, S. I.; Garcia-Garibay, M. A. *J. Org. Chem.* **2013**, *78*, 5293.
(4) (a) Vogelsberg, C. S.; Garcia-Garibay, M. A. *Chem. Soc. Rev.* **2012**, *41*, 1892. (b) Khuong, T. A. V.; Nuñez, J. E.; Godinez, C. E.; Garcia-Garibay, M. A. *Acc. Chem. Res.* **2006**, *39*, 413. (c) Horansky, R. D.; Clarke, L. I.; Winston, E. B.; Price, J. C.; Karlen, S. D.; Jarowski, P. D.; Santillan, R.; Garcia-Garibay, M. A. *Phys. Rev. B* **2006**, *74*, 054306. (d) Shima, T.; Hampel, F.; Gladysz, J. A. *Angew. Chem., Int. Ed.* **2004**, *43*, 5537. (e) Lang, G. M.; Shima, T.; Wang, L.; Cluff, K. J.; Skopek, K.; Hampel, F.; Blümel, J.; Gladysz, J. A. *J. Am. Chem. Soc.* **2016**, *138*, 7649. (f) Setaka, W.; Yamaguchi, K. *J. Am. Chem. Soc.* **2012**, *134*, 12458. (g) Setaka, W.; Yamaguchi, K. *J. Am. Chem. Soc.* **2013**, *135*, 14560. (h) Akutagawa, T.; Koshinaka, H.; Sato, D.; Takeda, S.; Noro, S.-I.; Takahashi, H.; Kumai, R.; Tokura, Y.; Nakamura, T. *Nat. Mater.* **2009**, *8*, 342. (i) Yao, Z. S.; Yamamoto, K.; Cai, H. L.; Takahashi, K.; Sato, O. *J. Am. Chem. Soc.* **2016**, *138*, 12005. (j) Bracco, S.; Castiglioni, F.; Comotti, A.; Galli, S.; Negroni, M.; Maspero, A.; Sozzani, P. *Chem. Eur. J.* **2017**, *23*, 11210. (k) Commotii, A.; Bracco, S.; Yamamoto, A.; Beretta, M.; Hirukawa, T.; Tohnai, N.; Miyata, M.; Sozzani, P. *J. Am. Chem. Soc.* **2014**, *136*, 618.
(5) (a) Dominguez, Z.; Khuong, T. A. V.; Sanrame, C. N.; Dang, H.; Nuñez, J. E.; Garcia-Garibay, M. A. *J. Am. Chem. Soc.* **2003**, *125*, 8827. (b) Dominguez, Z.; Dang, H.; Strouse, M. J.; Garcia-Garibay, M. A. *J. Am. Chem. Soc.* **2002**, *124*, 2398. (c) Godinez, C. E.; Zepeda, G.; Garcia-Garibay, M. A. *J. Am. Chem. Soc.* **2002**, *124*, 4701. (d) Jarowski, P. D.; Houk, K. N.; Garcia-Garibay, M. A. *J. Am. Chem. Soc.* **2007**, *129*, 3110.
(6) Jobbaǵy, C.; Deaḱ, A. *Eur. J. Inorg. Chem.* **2014**, *2014*, 4434.
(7) (a) Balch, A. L. *Gold Bull.* **2004**, *37*, 45. (b) Pyykkö, P. *Angew. Chem., Int. Ed.* **2004**, *43*, 4412. (c) Katz, M. J.; Sakai, K.; Leznoff, D. B. *Chem. Soc. Rev.* **2008**, *37*, 1884. (d) Schmidbaur, H.; Schier, A. *Chem. Soc. Rev.* **2008**, *37*, 1931. (e) Laguna, A. Modern Supramolecular Gold Chemistry; Wiley-VCH; John Wiley distributor: Weinheim, Germany, **2008**. (f) Chen, Y.; Cheng, G.; Li, K.; Shelar, D. P.; Lu, W.; Che, C.-M. *Chem. Sci.* **2014**, *5*, 1348. (g) Ito, H.; Muromoto, M.; Kurenuma, S.; Ishizaka, S.; Kitamura, N.; Sato, H.; Seki, T. *Nature Communications* **2013**, *4*, 2009. (h) Seki, T.; Sakurada, K.; Ito, H. *Angew. Chem., Int. Ed.* **2013**, *52*, 12828. (i) Seki, T.; Sakurada, K.; Muromoto, M.; Ito, H. *Chem. Sci.* **2015**, *6*, 1491.
(8) Zalesskiy, S. S.; Sedykh, A. E.; Kashin, A. S.; Ananikov, V. P. *J. Am. Chem. Soc.* **2013**, *135*, 3550–3559.
(9) Macho, V.; Brombacher, L.; Spiess, H. W. *Appl. Magn. Reson.* **2001**, *20*, 405.
(10) (a) Laposa, J.D.; Singh, H. *Chem. Phys. Lett.* **1969**, *4*, 288. (b) Emmert, L.A.; Choi, W.; Marshal, J.A.; Yang, Y.; Meyer, L.A.; Brozic, J.A. *J. Phys. Chem. A* **2003**, *107*, 11340. (c) Chao, H.Y.; Lu, W.; Li, Y.; Chan, M.C.W.; Che, C.-M.; Cheung, K.-K.; Zhu, N. *J. Am. Chem. Soc.* **2002**, *124*, 14696.
(11) It has been shown that structures analogous to **1** can display phosphorescence emission in solution by photoactivated removal of oxygen: Wan, S.; Lu, W. *Angew. Chem. Int. Ed.* **2017**, *56*, 1784.
(12) Levitus, M.; Zepeda, G.; Dang, H.; Godinez, C.; Khuong, T. A. V.; Schmieder, K.; Garcia-Garibay, M.A. *J. Org. Chem.* **2001**, *66*, 3188.
(13) Krämer, M.; Bunz, U.H.F.; Dreuw, A. *J. Phys. Chem. A*, **2017**, *121*, 946.
(14) (a) Levitus, M.; Schmieder, K.; Ricks, H.; Shimize, K.D.; Bunz, U.H.F; Garcia-Garibay, M.A. *J. Am. Chem. Soc.* **2001**, *123*, 4259. (b) Levitus, M.; Garcia-Garibay, M.A. *J. Phys. Chem. A* **2000**, *104*, 8632, (c) Yang, J.-S.; Yan, J.L.; Hwang, C.-Y; Chiou, S.-Y.; Liau, K.-L.; Tsai, H.H.G. Lee, G.S.; Peng, S.M. *J. Am. Chem. Soc.* **2001**, *123*, 4259.
(15) Cardolaccia, T.; Li, Y.; Schanze, K.S. *J. Am. Chem. Soc.* **2008**, *130*, 2535
(16) Yang, J.-S.; Yan, J.L.; Liau, K.-L.; Tsai, H.H.G.; Hwang, C.-Y. J. *Photochem. Photobiol. A: Chemistry*, **2009**, *207*, 38.
(17) Wang, L.; Li, Y.; Zhang, Y.; He, H.; Zhang, J. *Spectrochim. Acta Mol. Biomol. Spectrosc.* **2015**, *137*, 259.

Insert Table of Contents artwork here